β-particle energy-summing correction for β-delayed proton emission measurements

Z. Meisel[a,b,*], M. del Santo[b,c], H.L. Crawford[d], R.H. Cyburt[b,c], G.F. Grinyer[e], C. Langer[b,f], F. Montes[b,c], H. Schatz[b,c,g], K. Smith[b,h]

[a]*Institute of Nuclear and Particle Physics, Department of Physics and Astronomy, Ohio University, Athens, OH 45701, USA*
[b]*Joint Institute for Nuclear Astrophysics – Center for the Evolution of the Elements, www.jinaweb.org*
[c]*National Superconducting Cyclotron Laboratory, Michigan State University, East Lansing, MI 48824, USA*
[d]*Nuclear Science Division, Lawrence Berkeley National Laboratory, Berkeley, CA 94720, USA*
[e]*Grand Accélérateur National d'Ions Lourds, CEA/DSM-CNRS/IN2P3, Caen 14076, France*
[f]*Institute for Applied Physics, Goethe University Frankfurt am Main, 60438 Frankfurt am Main, Germany*
[g]*Department of Physics and Astronomy, Michigan State University, East Lansing, MI 48824, USA*
[h]*Department of Physics and Astronomy, University of Tennessee, Knoxville, TN 37996, USA*

Abstract

A common approach to studying β-delayed proton emission is to measure the energy of the emitted proton and corresponding nuclear recoil in a double-sided silicon-strip detector (DSSD) after implanting the β-delayed proton-emitting (βp) nucleus. However, in order to extract the proton-decay energy, the measured energy must be corrected for the additional energy implanted in the DSSD by the β-particle emitted from the βp nucleus, an effect referred to here as β-summing. We present an approach to determine an accurate correction for β-summing. Our method relies on the determination of the mean implantation depth of the βp nucleus within the DSSD by analyzing the shape of the total (proton + recoil + β) decay energy distribution shape. We validate this approach with other mean implantation depth measurement techniques that take advantage of energy deposition within DSSDs upstream and downstream of the implantation DSSD.

Keywords:
β-delayed proton emission; GEANT4; DSSD
PACS: 29.30.Ep, 29.40.Wk

1. Introduction

β-delayed proton emission experiments can be used to populate proton-emitting states in nuclei which are otherwise difficult to access. Such proton-emitting states can be of interest to nuclear astrophysics and nuclear structure studies [1–3]. Rare-isotope beam facilities that produce short-lived isotopes either by projectile fragmentation or using the isotope separation online (ISOL) technique provide the opportunity to study the exotic nuclei which exhibit β-delayed proton emission, βp nuclei.

To date, the most common method for studying βp nuclei employs the production of nuclei via projectile fragmentation followed by the subsequent implantation of the βp nucleus into a double-sided silicon-strip detector (DSSD) with a thickness on the order of 50-1000 μm [e.g. References 1, 2, 4–7]. After implantation into the DSSD, the βp nucleus undergoes β-delayed proton emission and the energy of the proton and the corresponding nuclear recoil (referred to here as the proton-decay energy) is then detected within the DSSD. The high degree of segmentation

in the DSSD, in the case studied here forty 1 mm-pitch strips in both planar dimensions, enables the correlation of implants and decays, even with implantation rates on the order of 1 kHz. This capability has the advantage of turning the contaminant nuclei in the beam whose decays are well understood into calibration nuclei.

One consequence of using the projectile fragmentation production method is a relatively large energy spread of the ions of interest that impinge on the implantation DSSD. This large energy spread requires a relatively thick DSSD to stop all ions of interest in the active area of the detector. However, an undesired consequence of this approach is the additional energy deposited in the DSSD from the β-particle which is emitted almost simultaneously with the proton in β-delayed proton emission. Therefore what is measured is not the proton-decay energy, but rather the total decay energy. This is a phenomenon we refer to here as the β-summing effect. An example in the literature is shown in Figure 8 of Reference [4], where it is evident that the Gaussian peak of proton energy deposition is shifted to higher energy and convolved with a high-energy tail due to the addition of β-particle energy deposition. The β-summing effect is one of the dominant uncertainties in determining the energy deposited by a proton decay within a

*Corresponding author
Email address:* `meisel@ohio.edu` (Z. Meisel)

DSSD after a β-delayed proton emission event, contributing several tens of keV to energy uncertainties of $\sim$50–100 keV for proton-decay energies of a few MeV [1, 5]. As such, it is necessary to take into account β-summing for studies of βp nuclei whose results rely on a precise proton-decay energy determination, which is often the case for nuclear astrophysics [e.g. Reference 1].

We present here an approach to addressing the problem of β-summing. This method, which was employed in the analysis of data presented in Reference [1], consists of determining the mean implantation depth of a βp nucleus within a DSSD by reproducing the measured shape of the total (proton + recoil + β) energy-deposition histogram for β-delayed proton-emission events with simulations. The following section, Section 2, discusses the data collected and GEANT4 [8] simulations used to accomplish the β-summing correction analysis, as well as the simulation validation. Section 3 presents our newly developed mean implantation depth determination method, which is essential in determining the β-summing correction, and Section 4 provides comparisons to alternative mean implantation depth determination methods. Section 5 describes the full process of obtaining the β-summing correction.
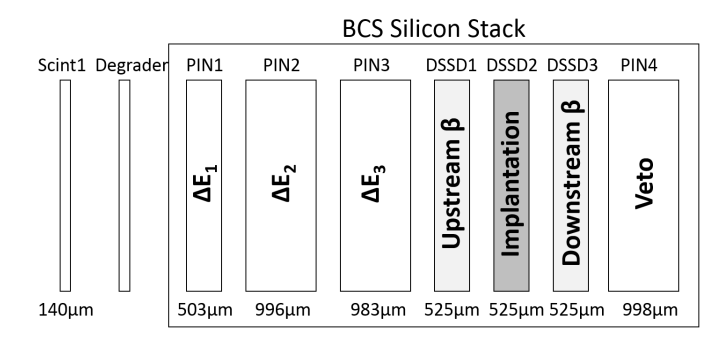
Figure 1: Schematic arrangement of the silicon detectors within the NSCL BCS in the configuration used for the experimental campaign described in the text. *Scint1* is a BC400 timing scintillator, *Degrader* is an aluminum foil, *PIN* are single-sided silicon strip detectors, and *DSSD* are double-sided silicon-strip detectors. The thickness of each detector is indicated below it in the figure and the role of each detector is indicated by the label within the detector. Relative longitudinal spacings of the detectors are listed in Table 1.

2. Measurements and Simulations

We focus on the β-summing correction which was developed using data from a β-delayed proton emission experimental campaign performed at the National Superconducting Cyclotron Laboratory (NSCL), partially described in Reference [1]. The data chosen are typical of that collected on βp nuclei produced via projectile fragmentation, with subsequent implantation into a relatively

Table 1: Thicknesses and relative longitudinal positions of the detectors' central planes (along the beam axis) with respect to DSSD2, the detector in which βp nuclei were implanted. See Figure 1 for a schematic representation.

Detector	Thickness [mm]	Relative position [mm]
PIN1	0.503	-7.73
PIN2	0.996	-5.87
PIN3	0.983	-3.68
DSSD1	0.525	-1.73
DSSD2	0.525	0.00
DSSD3	0.525	2.23
PIN4	0.998	4.19

thick DSSD. Additionally, properties of the studied nuclei are well known from previously published data. As such, they provide an ideal case to study our proposed β-summing correction method. GEANT4 [8] was chosen to simulate the measurements due to its flexibility and rigorously validated physics packages [e.g. Reference 9]. The following subsections provide detailed descriptions of the experimental data collection and the simulations thereof.

2.1. β-summing data collection

The data to assess β-summing were collected using βp emitting nuclei which were produced via projectile fragmentation using the Coupled Cyclotron Facility at the NSCL [10]. The primary beam used to produce the βp nuclei ^{23}Si and ^{20}Mg was ^{36}Ar, whereas a ^{78}Kr primary beam was used to produce the βp nucleus ^{69}Kr. The primary beams were impinged on a beryllium target of thickness 1060 mg/cm^2 for ^{36}Ar and 141 mg/cm^2 for ^{78}Kr at an energy of 150 MeV/u. The resultant cocktail beams were purified first with the A1900 fragment separator [11] and then further purified via the Radio Frequency Fragment Separator [12] prior to implantation within the central DSSD of the Beta Counting System (BCS) [13], where β-delayed proton emission events were measured. The implantation rate within the BCS was $\sim$100 Hz.

A schematic of the experiment set-up is given in Figure 1 and the relative longitudinal positions of detectors within the BCS are listed in Table 1. Particle identification of implanted nuclei was performed using the ΔE–TOF technique, where timing signals were provided by the Coupled Cyclotron RF and a 140 μm-thick BC400 scintillator upstream of the BCS and three PIN detectors, of thickness 503 μm, 996 μm, and 983 μm. The PIN detectors were also used to measure energy loss prior to the implantation DSSD. An aluminum degrader upstream of the BCS was used to ensure implantation of nuclei of interest within the central DSSD of the BCS by adjusting the degrader's angle with respect to the beam direction. A stack of three 525 μm DSSDs, model BB1 from Micron Semiconductor Ltd., located downstream of the first three PIN detectors in the BCS were used to detect implantations from beam fragments and β-particles from subsequent decays. The central DSSD was intended for implantation of βp nuclei.

A single 998 μm-thick PIN detector, located downstream of the DSSD stack within the BCS, was used to veto light beam fragments that could be mistaken for β-particles by rejecting events with a coincident upstream PIN detection. Each DSSD is segmented into 40×40 strips with a 1 mm pitch, i.e. consisting of 1600 1×1 mm^2 virtual pixels. Each PIN detector is 5×5 cm^2 and has no segmentation. The detectors within the BCS were surrounded by the Segmented Germanium Array (SeGA) in the beta-configuration [14] in order to measure proton emission branchings and decays to non-proton-emitting states with high resolution.

β-delayed proton emission events were correlated in time with βp nuclei previously implanted in the same DSSD pixel, while SeGA provided complementary γ-detection. A notable contaminant which accompanied the βp nucleus ^{69}Kr was ^{67}Se (See Figure 2 of Reference [1].), as this was used to determine the implantation DSSD detection threshold (See Section 2.3.). Before and after the projectile fragmentation experiments, the calibration α-source ^{228}Th was employed to characterize the energy resolution of the DSSDs.

2.2. GEANT4 simulations

We employ the Monte Carlo particle transport software GEANT4 [8] version 9.6.02 to simulate the β-delayed proton emission measurements described in the previous subsection. Detector features such as geometry, orientation, and resolution were included in the GEANT4 simulations, though for the purpose of simplification the BCS was modeled as a stack of free-floating silicon detectors within an aluminum cylinder.

β-energy spectra were sampled from the β-decay distribution given by the Fermi theory of β-decay [15], defined by the Q-value between the initial and final states. Strictly speaking, the final shape of the β-decay energy distribution depends on nuclear corrections related to the charge and size of the parent nucleus [16–20]. However, these higher-order nuclear corrections result in a relatively minor change (e.g. compared to small changes in the decay Q-value) in the overall decay spectrum shape [21, 22] and so these nuclear corrections can be safely neglected. Though the Q-value significantly affects the energy spectrum of emitted β-particles, we demonstrate (in Section 2.4) a relatively small sensitivity of our reported results to the choice of β-decay Q-value, which could vary due to mass uncertainties and/or different assumed final states of the decay.

2.3. Simulation validation

Since a proton from an implanted βp nucleus with an energy up to a few MeV has a mean free path up to tens of microns[1], it generally deposits 100% of its energy within the DSSD, as does the corresponding nuclear recoil, and therefore the critical element of the GEANT4 simulations requiring validation is the partial energy deposition of the

β-particle within the DSSD. The simulation of β-particle energy deposition within the DSSD was validated via comparison to experimental measurements of the well-studied β-emitter ^{67}Se [23], which accompanied the production of ^{69}Kr as a contaminant from fragmentation of ^{78}Kr (Shown in Figure 2 of Reference [1].).

Comparison to data required a determination of the energy resolution and energy detection threshold of the implantation DSSD. The 150 keV FWHM energy resolution, which was observed to be dominated by electronic noise and thus independent of energy, was determined by fitting several Gaussian distributions to the spectrum of a ^{228}Th α-source. We used a probabilistic criterion to mimic the analog-to-digital-converter (ADC) detection threshold (which is not a fixed energy due to electronic variations that affect the conversion from deposited energy to a voltage), where we used the acceptance-rejection method [24] to sample from an ansatz[2] for the likelihood of crossing the ADC threshold, given by the following equation,

$$\text{threshold(E)} = 0.5 \left(1 + \tanh \left(\frac{\text{E} - \text{c}}{\text{d}} \right) \right), \quad (1)$$
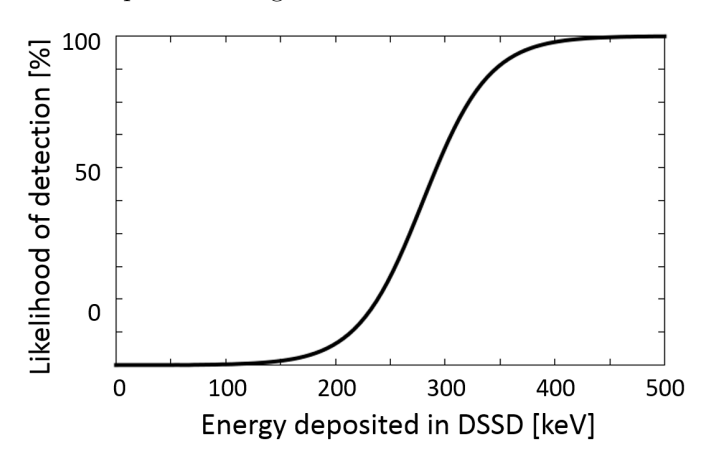
which is plotted in Figure 2.

Figure 2: Likelihood of event detection as a function of energy deposited within the implantation DSSD, as given by Equation 1 with c=60 keV and d=280 keV.

The two free parameters of Equation 1 used to mimic the β detection threshold for a β-particle with energy E, namely the diffuseness d and centroid c of the hyperbolic tangent, were determined via a χ^2-minimization comparison between simulations and data for ^{67}Se β-decays to

---

[2]The chosen functional form for the threshold function was motivated by the fact that electronic noise accompanying our energy signals is presumed to be due to a convolution of many random factors, which, via the central limit theorem, one would expect to contribute a Gaussian fluctuation to our energy-signal amplitude. The probability of crossing the ADC threshold would then be given by the integral of a normal distribution, i.e. the error function, centered about the threshold mean. To enable a fit to data, instead a similar function that is also in the class of sigmoid functions, but with a simpler functional form, namely the hyperbolic tangent, was chosen instead.

be 60 keV and 280 keV, respectively. Equation 1 was applied to a `GEANT4` simulation of ^{67}Se β-decays distributed within a 525 μm-thick DSSD that mirrored the experimental conditions for the ^{67}Se β-decay measurement discussed in Section 2.1 (Also described in Reference [1].). The simulated location in the DSSD for the ^{67}Se β-decay was sampled from a fit to data for the implantation planar position and from a depth distribution calculated with `LISE++` [25]. Following the acceptance-rejection method, the β-energy E, which was sampled in a Monte Carlo fashion from the β-energy distribution for ^{67}Se, was then used as input to Equation 1. The result of this calculation was compared to a randomly generated number using a box-like uniform distribution. This was used to decide whether a β-particle was 'detected' or discarded. The simulation results were in good agreement with the experimental data, as seen in Figure 3. We note that the fraction of rejected events with respect to recorded events for the `GEANT4` simulation, 66%, was in agreement with the experimentally measured ratio of detected ^{67}Se implants to detected ^{67}Se β-decays, roughly 68%.
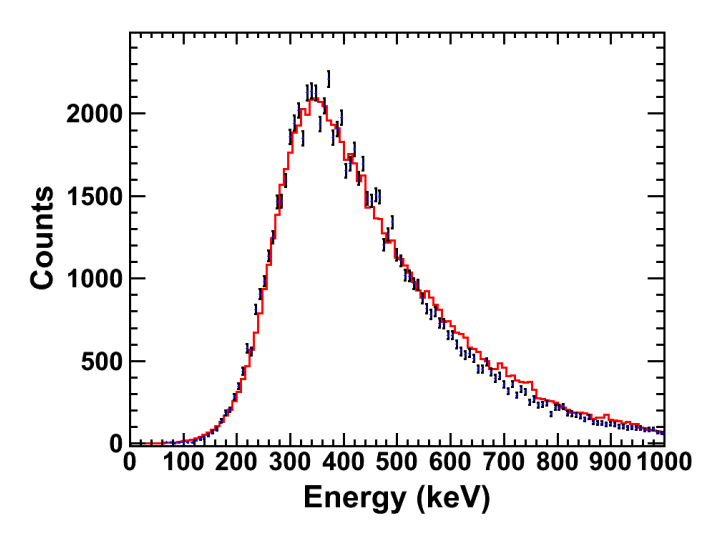
Figure 3: (color online.) Comparison of energy deposited by ^{67}Se β^{+}-decays implanted in a 525 μm-thick DSSD as simulated by `GEANT4` (solid line) and measured (points), where a detection threshold given by Equation 1 with $d = 60$ keV and $c = 280$ keV has been applied to the `GEANT4` spectrum. A detector resolution of 150 keV FWHM has been applied to the simulation data. Note that the simulation and data have the same binning, where the area of the simulation has been scaled to match the data.

For the DSSD energy-calibration we used a ^{228}Th α-source, providing energies E_α =5.400, 5.685, 6.288, and 6.778 MeV [26], and known β-delayed protons from ^{20}Mg, $E_{\rm p}$ =0.806, 1.679, and 2.692 MeV [6]^3, and ^{23}Si, $E_{\rm p}$ =1.32, 2.40, 2.83, and 3.04 MeV [7], which were ^{36}Ar fast-beam

---

^{3}The first two proton-decay energies have been measured to higher-precision by [27]. The results are consistent with [6] (whose energies were used for this work and the corresponding work [1]) within uncertainties and therefore would not impact the reported results.

fragments measured within the implantation DSSD. Note that the use of measured energies from β-delayed protons from ^{20}Mg and ^{23}Si as calibration points required the β-summing correction (discussed in Section 5) to be applied. The uncertainty of the proton energies from βp emitters ^{20}Mg and ^{23}Si, which ranged from 15-60 keV, included a systematic uncertainty associated with the β-summing present in published studies [6, 7] that determined the proton-decay energies. References [6] and [7] each corrected for β-summing, however they do not elaborate on precisely how this was done.
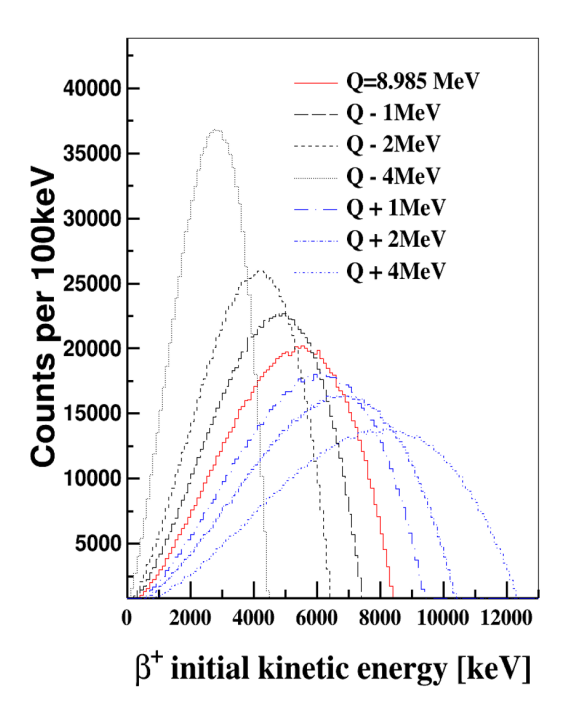
2.4. Sensitivity to decay Q-value

Though the reported β-summing correction technique relies on knowing the β-energy spectrum, we demonstrate that our results are relatively insensitive to uncertainties in the β-decay Q-value, where here the Q-value is to the final state and not necessarily the ground state.

The employed Q-values in this work were 9073 keV for ^{67}Se [28] (where a 100% branch to the ground state was assumed), 6686 keV for the ^{20}Mg decay branch to the proton emitting state of ^{20}Na at 806 keV [6, 28], 12083 keV for the ^{23}Si decay branch to the proton emitting state of ^{23}Al at 2400 keV [7, 28], 12655 keV for the ^{69}Kr decay to the ^{69}Br ground state [1, 28], and 9502 keV for the ^{69}Kr decay to the proton emitting state of ^{69}Br at 2940 keV [1, 28, 29]. Since the simulations were performed for the analysis presented in Reference [1], a more recent mass evaluation has been published [30]. In no case does the resultant updated Q-value differ from the Q-value employed in this work by more than 90 keV.

`GEANT4` simulations were performed for the ^{67}Se β-decay, modifying the Q-value from Reference [30] by several MeV in order to mimic β-decay channels into excited states of the daughter. Though the initial β-energy spectra varied dramatically, the spectra for β-energy deposition within the DSSD were remarkably similar for large modifications to the initial Q-value, as shown in Figure 4. In fact, the β-energy deposition spectra were nearly indistinguishable, except for the simulation which employed a Q-value reduced by 4 MeV from the nominal value of $\sim$9 MeV. This insensitivity to relatively substantial modifications of the decay Q-value is not surprising, but rather expected upon inspection of the analytic relation for energy deposition of β-particles in solid media. Figure 5 shows the relation taken from Reference [31] for β-energy deposition within 260 μm of silicon for β-particles ranging from 0.1-13 MeV. There, it is apparent that β-particles over an energy span of $\sim$2-13 MeV are expected to deposit nearly the same amount of energy when traveling through the same thickness of silicon. Therefore, sensitivity to the Q-value, due to the choice of decay final state or the state's energy uncertainty, is not expected for Q-values which result in a mean initial β-energy over $\sim$2 MeV, i.e. $Q \gtrsim 5$ MeV. Since all of the Q-values for the decays under consideration in this study are over this threshold (and in all cases the
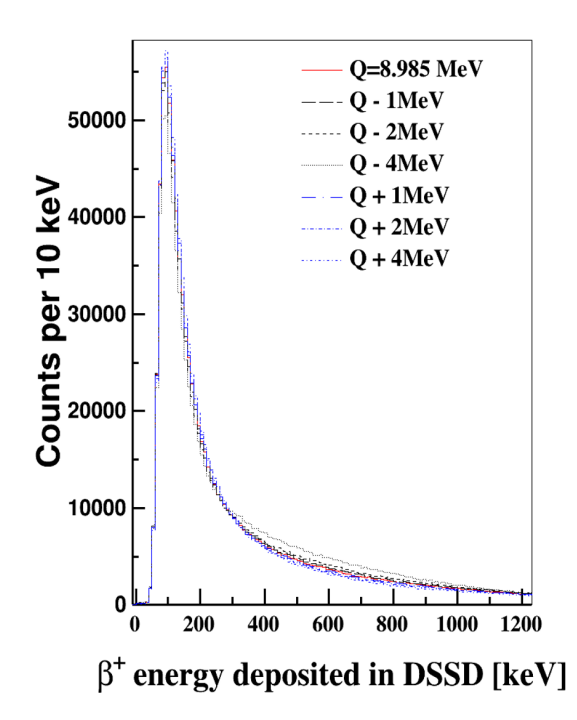
Figure 4: (color online.) GEANT4 simulation results (omitting detector threshold and resolution effects) for ^{67}Se β-decays, modifying the Q-value by up to ± 4 MeV from the nominal value of ~ 9 MeV. The left panel shows the initial β-energy spectra, while the right panel shows the corresponding β-energy deposited within the implantation DSSD.

Q-value uncertainty is 0.5 MeV or less), we do not expect the choice of Q-value for our simulations to impact the results for the β-energy deposition and therefore for β-summing. This insensitivity to the Q-value ultimately allows a higher-statistics β-delayed proton emission decay branches to be used to determine the β-summing correction for a lower-statistics decay branch with a roughly similar Q-value, as was done for ^{69}Kr in Reference [1].
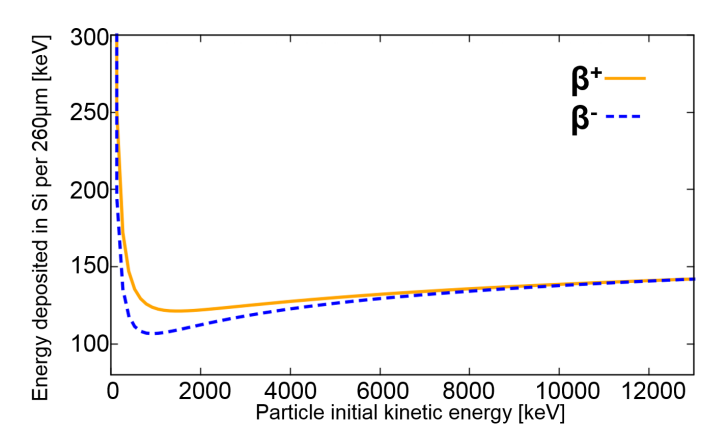
Figure 5: (color online.) Analytic energy deposition of β^+ (solid orange line) and β^- (dashed blue line) particles, using the relations from Reference [31], in a 260 μm-thick layer of silicon.

3. Novel implantation depth determination method

The amount of β-summing which occurs for a given βp emission depends sensitively on the depth within the DSSD at which the βp emission occurs. A deeper depth within the DSSD implies that the emitted β travels through more material while escaping the implantation DSSD and thus deposits more energy, on average, when compared to a βp emission at a shallower depth. Though the stochastic nature of implantation depth and β energy-loss reduces the strength of the previous statement, it remains true for an ensemble of βp emissions. Thus, the determination of the mean implantation depth of a βp emitter substantially reduces the uncertainty associated with implementing the β-summing correction for proton-energy determination. Typically, the two available methods for determining implantation depth, described in the following section (Section 4), are dependent on the energy calibration of three DSSDs and similar response to β-particles of the same energy for two DSSDs. Instead, our method, which is outlined in this section, relies on the energy calibration of only a single DSSD. Note that the insensitivity to the detector threshold is true for the majority of β-delayed proton emission experiments since proton energies are usually $\gtrsim 1$ MeV, while the detection threshold plays no role above ~ 0.5 MeV, as seen in Figure 2. Consequently, our method provides an efficient way to minimize systematic uncertainties present for the β-summing correction.

In simulating β-delayed proton emission, we include the energy and angle of the decay products and the position of the βp-emitter within the DSSD, each of which

is sampled from a probability distribution event-by-event. We sample the positron energy from the β-decay distribution given by the Fermi theory of β-decay [15]. Corrections for detector threshold and resolution are applied to the discrete proton energy and deposited β energy. The distributions for proton and positron emission angles are isotropic, since the orientations of nuclei stopped within the DSSD are random. The β-decay position on the plane of the DSSD that is perpendicular to the beam-direction is selected from a two-dimensional skew Gaussian which was fitted to the measured implantation distribution, which was possible due to the segmentation of the DSSD into virtual pixels. As the implantation depth for a given β-delayed proton emission event is *a priori* unknown, due to the lack of segmentation in the depth-dimension of the DSSD, the depth of the βp-emitter within the implantation DSSD is selected from a skew Gaussian distribution that is fitted to the implantation depth distribution simulated with the multi-purpose simulation tool LISE++ [25] (using their Straggling Method 1) for the β-delayed proton emission experiments discussed here. We stress that LISE++ is not able to accurately predict the absolute implantation depth of βp nuclei within the implantation DSSD, hence the need for the adjustable aluminum degrader upstream of the BCS (See Figure 1.), though we find it accurately predicts the relative separation in mean implantation depth for ions measured in the same projectile fragmentation experiment (See Section 4.). The implantation depth distributions for the simulated βp nuclei, shown in Figure 6, in general span roughly ⅓ of the 525 μm DSSD thickness. The widths of the distributions are due to the narrow momentum acceptance of the fragment separator, $\pm 0.07\%$ and $\pm 0.5\%$ for the ^{78}Kr and ^{36}Ar primary beams, respectively. The centroid of an implantation depth distribution is referred to here as the mean implantation depth. Figure 7 shows the impact of choosing different discrete depths (not sampling from a depth distribution) within the DSSD for β-delayed proton-emission events on energy deposition of β-particles emitted within the implantation DSSD.

The centroid of the depth distribution function from which the βp-implantation depth was sampled was changed in 5 μm steps from 0 to 260 μm between simulations, where these depths correspond to the upstream-face and center-plane of the DSSD, respectively. Due to the symmetry of the detector, equivalent results are obtained by choosing centroids from 525 to 265 μm. However, this degeneracy is not an issue, as an accurate β-summing correction only relies on knowing the distance between the centroid and closest DSSD planar surface. As will be shown in the following section, we find our mean implantation depth determination method has a precision on the order of tens of microns, and thus we find a 5 μm grid to be sufficient.

We find the profile of the histogram of energy deposition within the implantation DSSD is sensitive to the mean implantation depth, as demonstrated in Figure 7. Qualitatively, this can be understood by considering a single
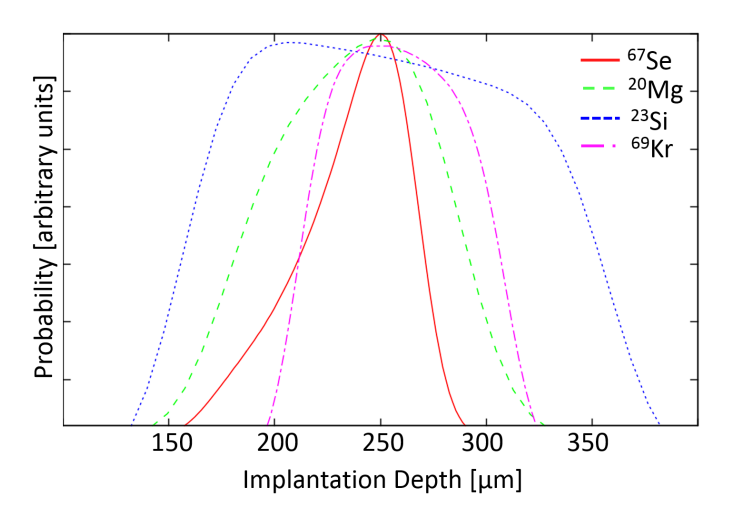

Figure 6: (color online.) Probability distributions for the implantation depths of ^{67}Se, ^{20}Mg, ^{23}Si, and ^{69}Kr ions within a 525 μm-thick DSSD calculated with LISE++ [25] using their Straggling Method 1. The amplitudes and centroids of each distribution have been shifted arbitrarily for comparison. The distribution shape is primarily related to the ion's momentum distribution, which depends on the ion production mechanism, e.g. target thickness and momentum-acceptance of the fragment separator through which the ion passes.

depth for β^+-emission, allowing a positron to be emitted within a given solid angle toward the downstream or upstream hemisphere of the DSSD, where the central plane of the DSSD defines the boundary between hemispheres, as in Figure 8. We justify this approximation made for the purpose of demonstration given the peaked nature of the βp-implantation depth distribution (FWHM ~ 0.15 mm) and the narrow thickness of the DSSD (0.525 mm) in comparison to its length and width (40×40 mm^2). From Figure 8 it is apparent that, by choosing a depth which is off-center, much more silicon is contained within a given solid angle for the thicker hemisphere as opposed to the thinner hemisphere. As energy deposition is linearly related to the length of detector traversed for a particle whose energy remains nearly constant, a condition which the positron roughly meets, it is apparent that the mean energy deposited will be higher for the events traversing the thicker hemisphere. For this simplified situation we obtain a low-energy peak for β-events in the hemisphere directed toward less silicon (closer to the surface) and a high-energy peak for β-events in the hemisphere directed toward more silicon (further from the surface). By considering the histograms obtained from each hemisphere together, we obtain double-peaked histograms like those shown in Figure 7. The high and low energy peaks are blended together by including the depth and β-energy distributions into the simulation, however the general effect remains.

To test our depth determination method, we use β-delayed proton emission of ^{20}Mg and ^{23}Si, each of which were produced via projectile fragmentation of ^{36}Ar and im-
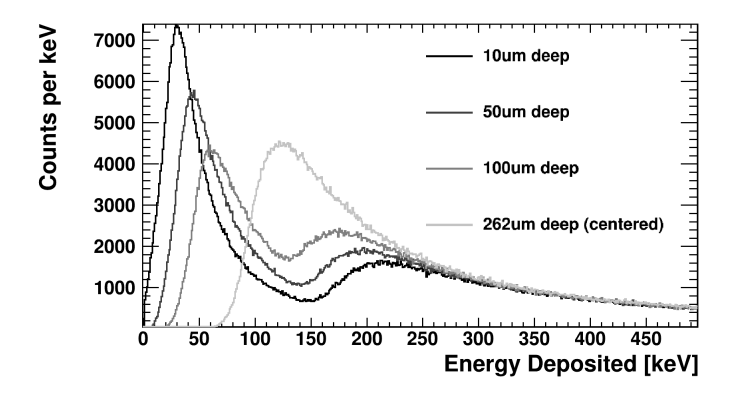
Figure 7: β-particle energy-deposition histograms from GEANT4 simulations of ^{67}Se β^+-emission at various depths within a 525 μm DSSD, where the detection threshold and detector resolution has not been applied. In each case the angular distribution of the β^+-emission was isotropic. Note that all simulated events originated from a single depth (indicated in the legend) and were not sampled from a depth distribution.

Figure 8: (color online.) Cartoon representation of a hypothetical β-particle emission (green circle) that occurs within a fixed solid angle (red areas) towards opposing DSSD (yellow rectangle) hemispheres. The relative average amount of material through which a β-particle travels changes depending on the location of the β-particle emission, thus affecting the energy-deposition spectrum, as seen in Figure 7.

planted in a 525 μm-thick DSSD[4]. For the proton-decay energy from each source with the highest statistics, $E_p = 0.806$ MeV for ^{20}Mg and $E_p = 2.40$ MeV for ^{23}Si, we perform our simulation for the aforementioned range of βp-implantation depth centroids and distributions. A reduced-χ^2 value is calculated for each mean implantation depth by comparing the simulated total (proton + recoil + β) energy deposition distribution to the data. The minimum of the fit to reduced-χ^2 results is taken as the mean implantation depth, whereas the uncertainty is the difference between this depth and the depth for which the fit to reduced-χ^2 results is +1 greater than the minimum. Figure 9 shows sample spectra comparing the total energy-deposition histogram of the 806 keV proton decay from ^{20}Mg to simulations using three different mean implantation depths. In this way we are able to assign a mean implantation depth for both ^{20}Mg and ^{23}Si (See Figure 10.), which we compare to other depth determination methods in the following section. The precise mean implantation depth is important because it corresponds to a reduction in the proton-decay energy uncertainty that results from the β-summing correction, as discussed in Section 5. This

---

[4]β-decay data were not used to assess the impact of implantation depth on β-summing since those data are far more sensitive to the DSSD detection threshold

method provides a way to determine the mean implantation depth of a βp emitter which can be used in addition to or in lieu of (if they are not feasible) the other methods of mean implantation depth determination discussed in the following section.
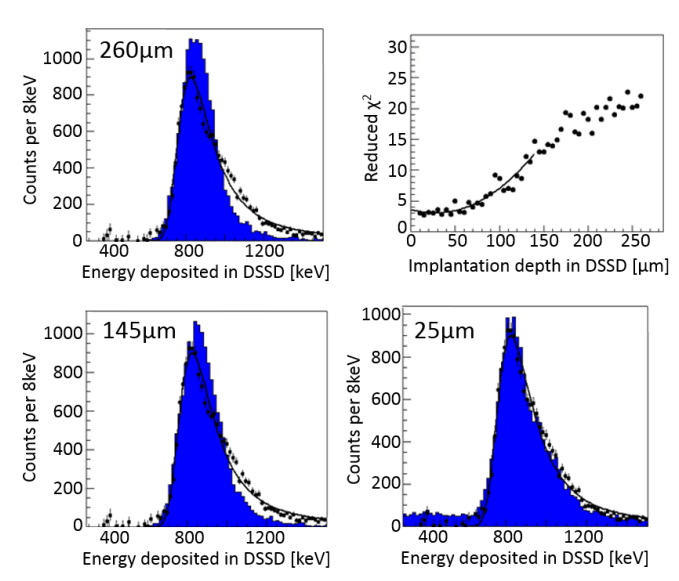

Figure 9: (color online.) Comparison between GEANT4 simulations (filled histogram) of ^{20}Mg total (proton + recoil + β) energy deposition corresponding to the 806 keV proton decay within a 525 μm-thick DSSD and experimental data (points) for simulated mean implantation depths of 260, 145, and 25 μm from the upstream planar surface of the implantation DSSD. The simulation histogram area has been scaled to match the data and a fit to data with a Landau distribution (black line) is included for reference. The upper-right panel contains the reduced-χ^2 between simulated total energy-deposition histograms and experimental spectra as a function of the βp nucleus mean implantation depth, including the quadratic fit.

4. Other mean implantation depth determination methods

In order to validate our mean implantation depth determination method, 'Method 1', we compare it to other available methods. In addition to the method described in the prior section, we use two independent methods to determine the mean implantation depth for the β-delayed proton emitters ^{20}Mg and ^{23}Si.

4.1. Method 2: Implantations per implantation DSSD and upstream or downstream DSSDs

For method 2 we look at the fraction of implantations of a given nucleus that occurs in the DSSDs which are neighbors to the implantation DSSD. This method requires that a nucleus is poorly centered within the central (implantation) DSSD in the BCS detector stack, and requires consideration of the asymmetry of the nucleus's implantation depth distribution. Integration is performed over the implantation depth probability distribution over the longitudinal range encompassing each DSSD until the fraction
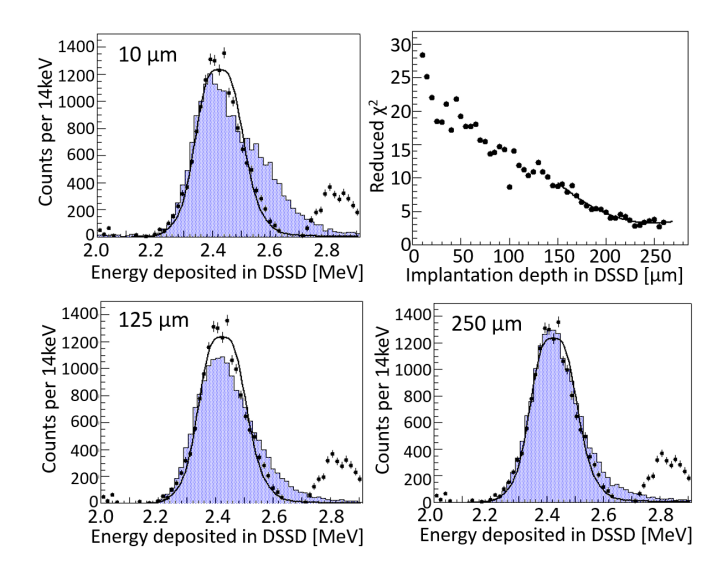
Figure 10: (color online.) Same as Figure 9, but for ^{23}Si βp events at mean implantation depths of 10, 125, and 250 μm. Note that the higher-energy peak in the data is from a separate proton-emitting branch.

of events occurring within each detector matches the fraction of implantation events observed for that nucleus in each DSSD. The uncertainty quoted for this method is the simulated mean implantation depth range for which the ratio of events deposited in the neighboring and implantation DSSDs agrees with the measured ratio within its statistical uncertainties.

This method is naturally more sensitive for nuclei whose mean implantation depth is close to the surface of the implantation DSSD, provided that nucleus has a narrow implantation depth distribution, and less sensitive (or impossible) for a nucleus well centered within the implantation DSSD. Since calculations of ^{20}Mg implantation with LISE++ [25] result in a depth distribution with FWHM 150 μm, whereas the DSSD is 525 μm-thick, this method works well. However, it is apparent that this implantation depth method is reliant on an accurate prediction of the implantation depth distribution shape.

4.2. Method 3: Mean β-energy difference between upstream and downstream DSSDs

For method 3, we compare the separation in mean energy deposited by positrons in the DSSDs which are upstream and downstream of the implantation DSSD (DSSD2 in Table 1), selecting only decays within a small solid angle about the axis perpendicular to the DSSD planes that correspond to the proton-emission channel of interest. Positrons which traveled through more silicon in the implantation DSSD on average lost more energy in the implantation DSSD than positrons which traveled through less silicon. Therefore, a slightly different β-energy deposition is expected between the DSSDs neighboring the implantation DSSD, since they are separated from the mean implantation depth by different amounts of silicon. This

Table 2: Mean implantation depth within a 525 μm-thick DSSD as determined by energy deposition profile χ^2-minimization, implantations per DSSD, and mean-energy difference between upstream and downstream DSSDs, which are termed Methods 1, 2, and 3, respectively. ^{23}Si has no value for Method 2 since all ^{23}Si nuclei were implanted within the central DSSD, i.e. DSSD2 in Table 1. It is apparent that Methods 1 and 3 are more precise for centrally-deposited βp nuclei, while Method 2 is preferred for βp nuclei deposited nearer to the surface of the implantation DSSD.

βp emitter	Method 1	Method 2	Method 3
^{20}Mg	27(36) μm	27(6) μm	61(50) μm
^{23}Si	250(40) μm	—	215(14) μm

phenomenon was used by Reference [6] to gate on events that had minimal β-summing in their implantation DSSD.
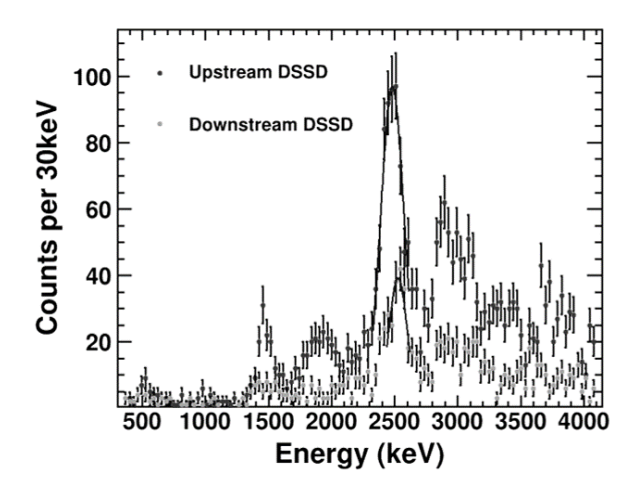
Simulations were employed to map between mean implantation depth and the mean β-energy deposition difference between β-energy distributions for the upstream and downstream DSSDs. The results of this process for ^{23}Si are shown in Figure 11, where the reported mean implantation depth uncertainty is the simulated depth range that resulted in an upstream-downstream mean β-energy difference within the range given by the fitted mean-energy uncertainties summed in quadrature. We note that this method of mean implantation depth determination relies upon the DSSDs which are upstream and downstream of the implantation DSSD having a similar response to β-particles of the same energy.

4.3. Comparison between mean implantation depth determination methods

We find agreement between each of the three mean implantation depth determination methods for ^{20}Mg and ^{23}Si, as seen in Table 2. The relative separation in mean implantation depth between ^{20}Mg and ^{23}Si is in good agreement with the separation predicted by LISE++, 180 μm. Here we stress that the advantage of the method presented in Section 3 (Method 1 of Table 2), is that it only requires a single DSSD, namely the implantation DSSD, and therefore is only sensitive to the energy calibration and electronic noise of one rather than three DSSDs and it is generally not sensitive to the detector threshold of any DSSD. Additionally, we note that Methods 1 and 3 are more precise for βp nuclei deposited closer to the center of the implantation DSSD, while Method 2 excels for βp nuclei deposited nearer to the implantation DSSD surface.

5. Determination of the β-summing correction

The accurate mean implantation depth determination methods described in the previous sections (Sections 3 and 4) enable an accurate determination of the average β-energy deposited in β-delayed proton emission events within a DSSD, and thus allow for an accurate proton-decay energy to be determined. The methods' typical precision of tens of microns results in an uncertainty in the
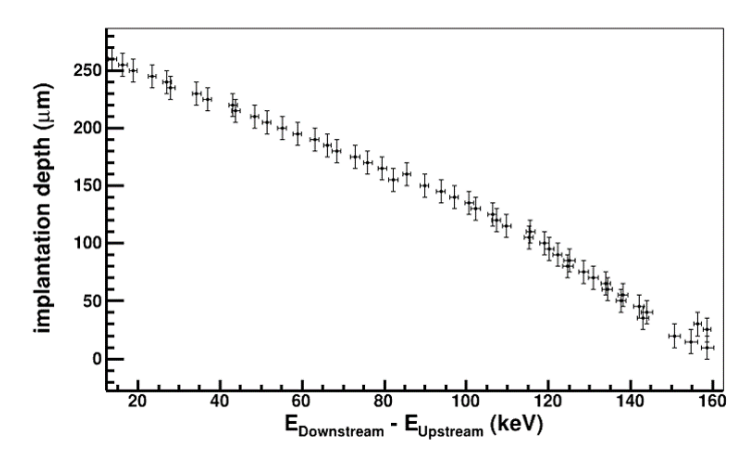
Figure 11: (color online.) Mean implantation depth determination 'Method 3' for ^{23}Si which used the difference in mean energy deposition within DSSDs upstream (dark-gray points) and downstream (light-gray points) of the implantation DSSD, where the blue lines are Gaussian fits (left panel) to β-energy deposition peaks associated with β-delayed proton emission of ^{23}Si through the proton-emission channel (E_p = 2.40 MeV) with the highest statistics. The left panel shows the energy distributions, whereas the right panel shows the energy difference between means of the upstream and downstream DSSD β-energy deposition distributions in relation to the implantation depth within the implantation DSSD for GEANT4 simulations. The measured mean-energy difference, $\langle E_{\mathrm{DSSD1}} \rangle - \langle E_{\mathrm{DSSD3}} \rangle = 45 \pm 9$ keV, corresponds to an implantation depth of 215±14 μm.

β-summing correction which is on the order of tens of keV for the cases presented here.

The relationship between β-summing and mean implantation depth within a 525 μm DSSD for ^{23}Si is shown in Figure 12. Under our conditions, an implantation depth distribution with ∼150 μm FWHM in a 525 μm-thick DSSD, we are able to determine the mean implantation depth within ∼40 μm; however, more accurate results would be possible for a narrower depth distribution in a thinner detector. As seen in Figure 12, the mean implantation depth uncertainty of 40 μm translates into a β-summing correction uncertainty of anywhere from 5 to 25 keV, depending on which place along the depth–correction relationship the mean implantation depth is located. Similarly for ^{20}Mg, whose β-summing correction was found to be between 10 and 85 keV depending on the mean implantation depth, the β-summing correction uncertainty was between 5 and 15 keV for the range of possible mean implantation depths. Given the determined implantation depth, the actual β-summing correction for the deduced mean implantation depth was 18±6 keV.

To correct for β-summing and determine the proton-decay energy from a β-delayed proton emitting nucleus, we incrementally iterate over proton-decay energies in the Monte Carlo simulation for each mean implantation depth. χ^2 minimization between the energy-deposition histograms, which include the energy deposited by the proton+recoil and β-summing, from the data and simulations simultaneously results in a proton-decay energy and mean implantation depth. This procedure has been used for the β-delayed proton emission of ^{69}Kr (using the 2.94 MeV proton-decay peak) to obtain a summing correction of 79±12 keV[1].

Therefore, the full process of applying the β-summing

correction to obtain a precise proton energy from a β-delayed proton emission measurement in a DSSD is the following:

1. Obtain the βp nucleus surface implantation distribution by fitting to the implantation distribution measured with the pixelated DSSD.
2. Obtain the βp implantation depth distribution by fitting to results from LISE++ simulations that mimic experimental conditions, i.e. ion production, transport, and detector materials.
3. Perform Monte Carlo simulations for a given β-delayed proton decay branch with GEANT4, randomly selecting the β energy and angle, proton angle, and βp decay location, for mean implantation depths ranging from the detector surface to detector center.
4. Perform χ^2-minimization between the simulated and measured total (proton + recoil + β) energy-deposition histograms, allowing the location of the histogram peak to vary.
5. For the simulation which yields the minimum reduced-χ^2, the location of the histogram peak simultaneously yields the proton-decay energy and the amount of β-summing (since the proton-decay energy deposited in the simulation can be plotted simultaneously with the total energy-deposition).

6. Conclusions

In summary, we present an approach to address the problem of β-summing in the measurement of proton-decay energies of β-delayed proton-emitting nuclei detected via
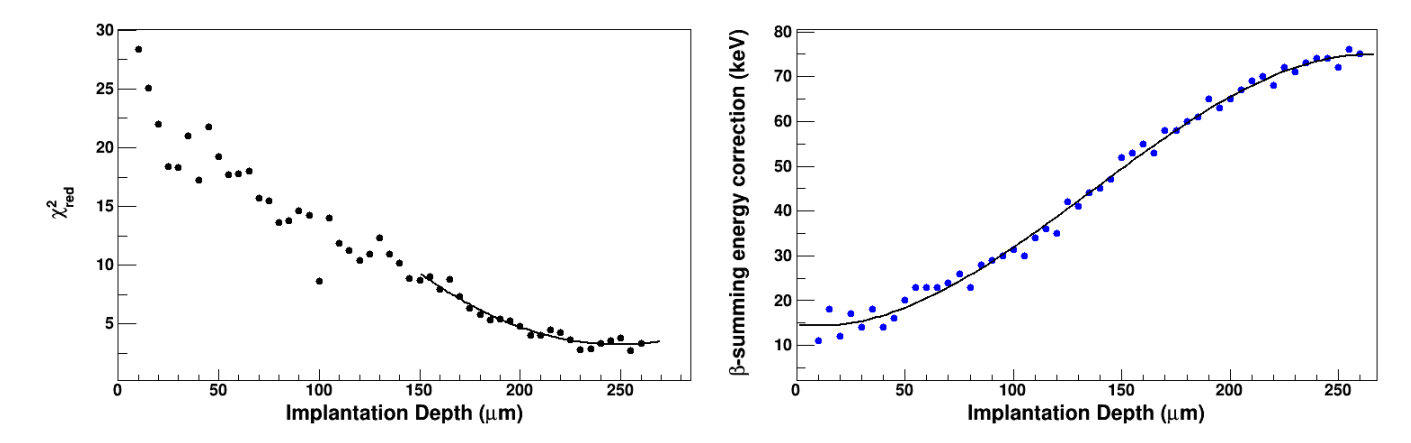
Figure 12: (color online.) Reduced-χ^2 minimization from mean implantation depth determination Method 1 for ^{23}Si as a function of mean implantation depth (left panel), including a quadratic fit, demonstrating a mean implantation depth of 250 ± 40 μm. The right panel shows the corresponding β-summing correction applied to ^{23}Si proton energy deposition peaks as a function of mean implantation depth, where a third-order polynomial fit is included to guide the eye.

implantation within a DSSD. We demonstrate that determination of the mean implantation depth of the βp nucleus within the implantation DSSD subsequently determines the magnitude of β-summing. We describe three methods to determine the mean implantation depth, two of which require DSSDs located upstream and downstream of the implantation DSSD and a third which depends only on the total (proton + recoil + β) energy-deposition histogram of the implantation DSSD and is generally insensitive to the detector threshold uncertainty. For the cases discussed, these techniques are capable of determining the mean implantation depth of a ~ 100 MeV/u βp nucleus within a $\sim$0.5 mm-thick DSSD to within tens of microns, corresponding to a β-summing correction uncertainty of $<$25 keV.

7. Acknowledgements

References

[1] M. del Santo, et al., Phys. Lett. B 738 (2014) 453.
[2] G. Lorusso, et al., Phys. Rev. C 86 (2012) 014313.
[3] M. J. G. Borge, Phys. Scripta 2013 (2013) 014013.
[4] A. Saastamoinen, et al., Phys. Rev. C 83 (2011) 045808.
[5] S. E. A. Orrigo, et al., Phys. Rev. Lett. 112 (2014) 222501.
[6] A. Piechaczek, et al., Nucl. Phys. A 584 (1995) 509.
[7] B. Blank, et al., Z. Phys. A Hadron Nucl. 357 (1997) 247.
[8] S. Agostinelli, et al., Nucl. Instrum. Meth. A 506 (2003) 250.
[9] M. Batic, G. Hoff, M. G. Pia, P. Saracco, G. Weidenspointner, IEEE T. Nucl. Sci. 60 (2013) 2934.
[10] R. C. York, et al., in: E. Baron, M. Liuvin (Eds.), Cyclotrons and Their Applications 1998, Institute of Physics Publishing, 1999, p. 687.
[11] D. J. Morrissey, B. M. Sherrill, M. Steiner, A. Stolz, I. Wiedenhoever, Nucl. Instrum. Meth. B 204 (2003) 90.
[12] D. Bazin, V. Andreev, A. Becerril, M. Doléans, P. F. Mantica, J. Ottarson, H. Schatz, J. B. Stoker, J. Vincent, Nucl. Instrum. Meth. A 606 (2009) 314.
[13] J. I. Prisciandaro, A. C. Morton, P. F. Mantica, Nucl. Instrum. Meth. A 505 (2003) 140.
[14] W. F. Mueller, J. A. Church, T. Glasmacher, D. Gutknecht, G. Hackman, P. G. Hansen, Z. Hu, K. L. Miller, P. Quirin, Nucl. Instrum. Meth. A 466 (2001) 492.
[15] E. Fermi, Z. Phys. 88 (1934) 161.
[16] M. E. Rose, Phys. Rev. 49 (1936) 727.
[17] A. Sirlin, Phys. Rev. 164 (1967) 1767.
[18] A. Sirlin, Phys. Rev. D 35 (1987) 3423.
[19] D. H. Wilkinson, Nucl. Instrum. Meth. A 275 (1989) 378.
[20] D. H. Wilkinson, Nucl. Instrum. Meth. A 290 (1990) 509.
[21] P. Venkataramaiah, K. Gopala, A. Basavaraju, S. S. Suryanarayana, H. Sanjeeviah, J. Phys. G. Nucl. Partic. 11 (1985) 359.
[22] E. A. George, P. A. Voytas, G. W. Severin, L. D. Knutson, Phys. Rev. C 90 (2014) 065501.
[23] H. Junde, H. Xiaolong, J. K. Tuli, Nucl. Data Sheets 106 (2005) 159 – 250.
[24] W. H. Press, S. A. Teukolsky, W. T. Vetterling, B. P. Flannery, Numerical Recipes, Cambridge University Press, Third edition, 2007.
[25] O. B. Tarasov, D. Bazin, Nucl. Instrum. Meth. B 266 (2008) 4657.
[26] A. Artna-Cohen, Nucl. Data Sheets 80 (1997) 227.
[27] J. P. Wallace, et al., Phys. Lett. B 712 (2012) 59.
[28] G. Audi, A. Wapastra, C. Thibault, Nucl. Phys. A 729 (2003) 337.
[29] A. M. Rogers, et al., Nucl. Data Sheets 120 (2014) 41.
[30] G. Audi, et al., Chin. Phys. C 36 (2012) 1287.
[31] F. Rohrlich, B. C. Carlson, Phys. Rev. 93 (1954) 38.